Journal of Hazardous Materials 432 (2022) 128755

Contents lists available at ScienceDirect

Journal of Hazardous Materials

journal homepage: www.elsevier.com/locate/jhazmat

Research Paper

Differential staining lowers the false positive detection in a novel volumetric measurement technique of microplastics

Abhrajyoti Tarafdar [1], Sang-Hyun Choi [2], Jung-Hwan Kwon [*,3]

Division of Environmental Science and Ecological Engineering, Korea University, 145 Anam-ro, Seongbuk-gu, Seoul 02841, Republic of Korea

HIGHLIGHTS

- Nile Red staining for detecting environmental and food microplastics.
- Removed most probable false detections using Calcofluor White, Evans Blue, and DAPI.
- Volumetric measurement of microplastics from Z-stack CLSM images.
- Regularly shaped microplastic materials were used to validate volumetric measurement.

GRAPHICAL ABSTRACT

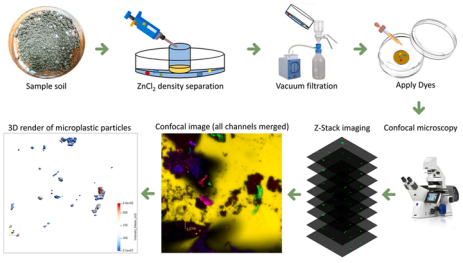

ARTICLE INFO

Editor: Teresa A.P. Rocha-Santos

Keywords:
Confocal microscopy
Z-stack CLSM
Microplastics volumetric measurement
Nile Red detection
Distinctive dyeing

ABSTRACT

A novel method for the volumetric detection of microplastics in various environmental (soil, water) and food (fish, meat) matrices was developed. The method is based on the Nile Red staining of microplastics while eliminating probable interference by other organic polymers such as lignin, chitin, cellulosic materials, and other organic substances using a mixture of three water-based dyes (Calcofluor White, Evans Blue, and 4,6-diamidino-2-phenylindole [DAPI]). The excitation/emission 'sweet spot' was determined for water based blue dyes to detect them in a single channel for effective elimination of probable contaminations. Detection of microplastic particles using the Nile Red method was validated by comparing with traditional detection of microplastics via Fourier transform infrared spectroscopy (FTIR). Volumetric measurements of the microplastics present in environmental samples were made possible using Z-stack confocal microscopy images backed by threshold-based 3D segmentation. Regularly shaped microplastic materials were used to validate the volumetric measurement method. The proposed volumetric determination method will be very useful for screening microplastics in diverse media and improving the prevailing method using FTIR.

Abbreviations: ABS, Acrylonitrile butadiene styrene; ATR-FTIR, Attenuated Total Reflection Fourier-transform infrared spectroscopy; CLSM, Confocal laser scanning microscopy; EPS, Expanded polystyrene; FTIR, Fourier-transform infrared spectroscopy; HDPE, High-density polyethylene; HPLC, High-performance liquid chromatography; LDPE, Low-density polyethylene; MBS, Main Beam Splitter; PA, Polyamide; PA-6, Polyamide 6 or Nylon 6; PBS, Polybutylene succinate; PC, Polycarbonate; PE, Polyethylene; PES, Polyester; PET, Polyethylene terephthalate; PEVA, Polyethylene vinyl acetate; PMT, Photo Multiplier Tube; PP, Polypropylene; PS, Polystyrene; PU, Polyurethane; PVC, Polyvinyl chloride; PVDF, Polyvinylidene fluoride; Pyro-GC/MS, Pyrolysis–gas chromatography–mass spectrometry; TGA-GC/MS, Thermogravimetric analysis–gas chromatography–mass spectrometry; VTK, Visualization Toolkit; WWTP, Wastewater Treatment Plant.

* Corresponding author.
E-mail address: junghwankwon@korea.ac.kr (J.-H. Kwon).
[1] ORCID: 0000-0003-0020-5279
[2] ORCID: 0000-0001-5817-3842
[3] ORCID: 0000-0002-6341-7562

https://doi.org/10.1016/j.jhazmat.2022.128755
Received 4 February 2022; Received in revised form 8 March 2022; Accepted 19 March 2022
Available online 23 March 2022

1. Introduction

The industrial manufacture of plastics appreciated outstanding development and this growth arrived at the worldwide yearly production of 367 million tons in 2020 (Plastics Europe & EPRO, 2021). At the current pace of development, this production has been assessed to be twofold and plastic waste streaming into the ocean will be tripled within the following two decades (Parker, 2020; World Economic Forum, 2016). During the year 2020, approximately 55 million tons of plastics were produced in Europe alone, while in the same year only approximately 10.2 million tonnes of waste plastics were recovered for recycling (Plastics Europe & EPRO, 2021). The ceaseless dumping of plastic waste has prompted expanded measures of microplastic defilement affecting the global environment. After entering the environment as waste, plastics can experience mechanical breakdown by weathering, prompting various shapes, sizes, and colors (Sridhar et al., 2022). Microplastics are polymers with particle sizes of less than 5 mm. Because of their tiny size, these human-generated wastes can be effectively assimilated by fauna and transferred to higher trophic levels in the food web (Lin et al., 2021). The existence of microplastics in an assortment of ecosystems should be assessed forthrightly because of the probable hazards they can possess (Tarafdar et al., 2021).

Several insightful strategies have been employed to measure or characterize microplastics in the environment; which incorporated ATR-FTIR (Alfonso et al., 2021; Piyawardhana et al., 2022; Uurasjärvi et al., 2021), Raman spectroscopy (Leung et al., 2021; Luo et al., 2021), pyrolysis–GC/MS (Ishimura et al., 2021; Picó and Barceló, 2020), and TGA-GC/MS (Liu et al., 2021). Spectrophotometric techniques, such as FTIR and Raman spectroscopy, help to count the number of microplastic particles and identify contaminated plastic types. However, uncertainty is associated with particle counts if the sample is larger in size/number, heterogeneous, and diverged. Again, spectrophotometric detection is limited to particle sizes smaller than 300 μm (Veerasingam et al., 2020). A longer detection time is also required (6–24 h per sample, excluding the time required for pre-treatments) for these methods (Hong et al., 2021). Sometimes plastic count is not sufficient to comprehend the depth of real contamination, as these detections are neither gravimetric nor volumetric (Liu et al., 2021). Thermo-analytical strategies, such as pyrolysis and TGA-GC/MS, can specifically separate and recognize plastic types. Qualitative and quantitative detection of microplastics is possible with these techniques at the sub-microgram level (Fischer and Scholz-Böttcher, 2017; Ye et al., 2021). Although a very small amount of the required test sample can influence the conclusion of the detection negatively, microplastics in the environment are not homogeneously distributed.

To resolve these problems, the latest application of fluorescence-directed recognition utilizing various dyes provided an approach to explicitly feature microplastics and differentiate them from minerals and organic remnants in the sample. This technique upgrades microplastic perception, recognition, and permits time-resolved estimation. The most commonly used stain to quantify microplastics based on fluorescence tagging is Nile Red (9-(diethylamino)-5H-benzo[*a*]phenoxazin-5-one). This dye is metachromatic, hydrophobic, and possesses adequate photochemical stability (Shruti et al., 2022). Nile Red has the advantage of rapid detection of microplastics, although it causes false positive detections for some organic debris because of its lipophilic nature (Shim et al., 2016). Another efficient rapid dyeing method was developed based on thermal expansion and contraction of polymers where three kind of fluorescent dyes (Safranine T, fluorescein isophosphate, and Nile red) were used to quantify microplastics (Lv et al., 2019).

In this study, we used a specific water-based blue dye mixture to identify the most probable false detections in a separate single-color channel of fluorescence detection. In addition to perfecting detection, this study also explored a novel volumetric method to quantify microplastics for the first time in virtually any matrix (soil, water, food, etc.), using a threshold-based 3D segmentation procedure on acquired Z-stack confocal images of microplastics.

2. Materials and methods

2.1. Materials

All microplastics used in this study were purchased in the form of pristine pellets from various chemical manufacturers (LDPE [grade: MB9500], HDPE [grade: ME2500], PP [grade: H1500], EPS [grade: B160], and PS [grade: 25SPI] from LG Chem Ltd., Seoul, Republic of Korea; PET [grade: Cool, KE-02328] from Lotte Chemical, Seoul, Republic of Korea; PU [product code: UR30-GL-000101] and PVDF [product code: FV30-GL-000100] from Goodfellow Cambridge Ltd., Huntingdon, UK). They were processed into fibers using a Dynisco LME (Franklin, MA, USA) and thereafter underwent cryogenic grinding using a 6875D Freezer/Mill® (Spex®SamplePrep, Metuchen, NJ, USA). The ground microplastics were sieved and particles of 100–300 μm were selected for experiments. All dyes (Nile Red [product no. 72485], Calcofluor White Stain [product no. 18909], and DAPI ready-made solution [product no. MBD0015]) were procured from Sigma-Aldrich (St. Louis, MO, USA). Sand and kaolinite were purchased from Fisher Scientific (Loughborough, UK), and peat moss was purchased from Premier (Riviere-du-Loup, Quebec, Canada). Zinc chloride used for density separation was purchased from Daejung Inc. (Siheung, Republic of Korea). Hydrogen peroxide (30%) used for peroxidation was purchased from J. T. Baker (Center Valley, PA, USA). All organic solvents (acetone, *n*-hexane, methanol, etc.) utilized in the dye solution and analysis were of HPLC grade and purchased from J.T. Baker and Daejung Inc.

2.2. Sample preparation and dyeing

To prepare the master microplastic mixture, the microplastic particles (LDPE, HDPE, PP, EPS, PS, PET, PU, and PVDF; particle size 100–300 μm) were mixed in equal weights. We also prepared a probable contamination mixture sample using shrimp shells, anchovy, cotton fibers, and wooden particles of equal weights (cryo-ground using Freezer/Mill®). Following the composition of artificial soil according to OECD test guidelines, an artificial soil sample composed of 75% sand (SiO_2), 20% kaolin clay ($H_2Al_2Si_2O_8$, H_2O), and 5% peat moss was prepared (OECD, 2010). For homogenization, peat moss was ground using a blender and sieved through a 2 mm sieve.

Nile Red dye (0.05 g L^{-1} in acetone, 10 times dilution in *n*-hexane) was utilized for the dyeing of microplastics. A water-based fluorescent dye solution (mixture of three dyes in proper ratio) was employed to detect the probable false positives obtained by the Nile Red staining method. Among the different false positives for microplastic detection using Nile Red method, natural polymers such as lignin, chitin, cellulosic materials, biofibers, insect-exoskeletons can be detected as false positives. In our dye solution, Calcofluor White (1 g L^{-1} Calcofluor White + 0.05 g L^{-1} Evans Blue) pigmented cellulosic biofibers, chitins, and insect exoskeletons (invertebrate remains). The fluorescence of Evans Blue is difficult to perceive along with Nile Red; nonetheless, it can be relied on to avoid some false positives from biological remnants (Helmberger et al., 2020). DAPI (4,6-diamidino-2-phenylindole) (10 μg mL^{-1}) is a nucleic acid stain that can cause fluorescence in any cell with nucleic acids, and thus, culminates in staining any organic contaminations from plants or animal bodies. All these dyes have similar excitation/emission ranges, which helps demonstrate probable contamination in a single blue channel of confocal microscopy.

For the sequential dyeing process, the samples were first mounted into a 35 mm glass-bottom confocal dish (SPL Life Sciences Co., Ltd., Pocheon, Republic of Korea). Then, 0.25 mL of blue dye solution (0.125 mL of Calcofluor White & Evan's blue solution along with 0.125 mL of DAPI) was applied to the sample and kept in the dark for 15 min. The excess dye was soaked off carefully using paper wipers (Kimtech Science

Wiper, Yuhan-Kimberly, Seoul, Republic of Korea). The samples were washed using Milli-Q water, soaked again using wipers, and dried in a vacuum desiccator (30 °C). After the completion of the process of applying blue dye solution, the Nile Red dye was applied (0.25 mL), followed by an *n*-hexane wash and drying in a vacuum desiccator (30 °C).

We also tested propidium iodide (PI) dye (Invitrogen, Carlsbad, CA, USA) to prompt fluorescence of dead (damaged membrane) cells (Fig. S1, Supplementary Material), which can act as a probable contaminant for Nile Red microplastic detection. Although both DAPI and propidium iodide are chromosome staining fluorochrome, their staining mechanisms differ in that DAPI is a DNA minor groove agent whereas propidium iodide acts as an intercalator. As these dyes have two different sites of attachment in the DNA, using them together can provide increased precision. However, we determined that it does not have any additional advantages over our Calcofluor White-Evans Blue-DAPI mixture practically.

Sample pretreatment comprised a two-step process involving organic removal and density separation. The first step in the analysis was the removal of organic matter with wet peroxidation with hydrogen peroxide (H_2O_2). We employed 30% H_2O_2 to digest the organic particles. A pre-weighed amount of artificial soil sample was added to a glass tube, and thereafter, 20 mL of aqueous 30% H_2O_2 solution was added. For the WWTP samples, 20 mL of water was aliquoted and added to a glass tube, followed by the addition of 30% H_2O_2. The glass tubes were wrapped with aluminum foil and the process was conducted in a clean bench to prevent any airborne contamination. Subsequently, the samples were heated in a dry oven at 65 °C for 3 h. Subsequent to wet peroxidation, any water content in the glass tubes was completely evaporated by heating at 80 °C. During evaporation, the samples were loosely covered with aluminum foil. Subsequent to the completion of wet peroxidation, density separation was performed using zinc chloride solution with a density of 1.78 g/mL to remove high-density particles such as sand and minerals. $ZnCl_2$ solution was freshly prepared each time and filtered before use through a glass fiber filter (GF/F, 0.7 μm, Whatman, UK). Further, 20 mL of $ZnCl_2$ solution was added to the glass tube, and microplastic particles were allowed to float near the surface overnight. Particles floating on the surface of the solution were overflown on a glass Petri dish containing excess $ZnCl_2$ solution in the glass tubes. The collected sample in the petri dish was filtered through a 20 μm stainless steel mesh filter under a vacuum pump. After filtration, the sample was secured in a clean glass dish to minimize potential contamination and stored away from humidity in a vacuum desiccator.

2.3. Field study

Agricultural fields with plastic sheet mulching and/or with a history of mulching were chosen for soil sampling (Fig. S6; Supplementary Material). These samples were investigated to demonstrate the suitability of the technique for natural field samples. A stainless steel augar was used to sample soil from a depth of less than 10 cm, which was collected in amber vials. Soil samples were dried in an incubator at 55 °C for 24 h. We used 2 mm mesh for sieving the soil to eliminate gravel. Density separation pretreatment was conducted on dried soil samples (1 g). Samples were stained sequentially prior to fluorescence imaging.

2.4. Comparison of CLSM with FTIR detection of microplastics

Wastewater samples were obtained from a municipal wastewater treatment plant (Fig. S8, Supplementary Material) with a daily capacity of 1590,000 m^3 day^{-1} in Seoul, Republic of Korea. This facility employs anaerobic-anoxic-aerobic (A2O) and Modified Ludzack Ettinger (MLE) treatment processes to efficiently remove organics and nutrients. For microplastics in WWTP influents, we submerged a stainless-steel bucket into the influent reservoir at a depth of 1 m and poured the collected water into a 4 L amber glass bottle.

Wastewater samples and two out of five artificial soil mixture sample were pretreated using wet peroxidation organic removal and subsequent ($ZnCl_2$) density separation. The remaining three artificial soil samples were not subjected to organic matter removal, and only density separation was performed to understand the effect of wet peroxidation in this comparison study. The blank was prepared by filtering water (Sigma Aldrich, HPLC grade) with a GF/F filter.

2.5. Detection methods for FTIR

Once microplastics were extracted through organic removal and density separation, an FTIR spectroscope equipped with a dissection microscope was utilized to perform the subsequent analysis steps (Nicolet iN10 MX; Thermo Fisher Scientific Inc., Waltham, MA, USA) to detect the microplastic particles. Spectroscopic analysis was performed in transmittance mode using a liquid nitrogen-cooled array detector, covering the IR spectral range of 4000–700 cm^{-1} with a spectral resolution of 16 cm^{-1} and a spatial resolution of 25 μm. Due to the limitations of the FTIR imaging analysis system, the area of the sample-holding-filters was divided into three areas and scanned. Once a spectral mapping image of the filter area containing the spectrum of the particle was generated, it was subsequently analyzed using the OMNIC Spectra program (Thermo Fisher Scientific Inc., OMNIC version 9) to count microplastics, to identify the polymer type, and to estimate their size. Spectra of the acquired particles were compared to the spectral reference database (Table S1, Supplementary Material) and were confirmed with a similarity or matching rate above 80%.

2.6. Fluorescence microscopic method

A Zeiss LSM 700 AxioObserver CLSM was used with Zeiss Zen 2012 software (Carl Zeiss, Oberkochen, Germany). A Plan-Apochromat objective (10x/0.45 W Korr M27) was used to digitally capture images (512 × 512 pixels, 1.28 × 1.28 mm, 8 bits) at × 10 magnification. The cover glass thickness was 0.17 mm. Filter wavelengths for each channel are hereinafter represented as: Channel-1: Nile Red (excitation wavelength 555 nm, emission wavelength 585 nm, and detection wavelength 600–800 nm), Channel-2: Nile Red (excitation wavelength 488 nm, emission wavelength 523 nm, and detection wavelength 490–550 nm), Channel-3: Calcofluor White + Evans Blue + DAPI (excitation wavelength 400 nm, emission wavelength 435 nm, and detection wavelength 300–440 nm). An MBS 405/488/555/639 beam splitter and a PMT detector were used. Green, orange, and blue gain/intensities were adjusted to denoise and to produce better visibility. After optimizing the CLSM adjustment settings, the same setup was maintained throughout the scanning of the test series. We collected some images (volumetric measurements) as a Z-stack series through the thickness of the sample with distances of 5 and 7 μm between slices; there were 15–22 slices (focal planes) per image. Maximum intensity orthogonal projection was employed to flatten the image for 2D visualization. Some of the images were also taken in tile scans (256 tiles) to cover a larger area (7038 × 7038 pixels, 15.79 × 15.79 mm).

2.7. Volumetric analysis of detected microplastics

Z-Stack Carl Zeiss Image (.czi) files generated by the CLSM instrument were processed using BiofilmQ (Hartmann et al., 2021) software to calculate the volume for each fluorescence channel. The images were denoised using convolution. Top-Hat filtering was applied to remove background fluorescence and fluorescence between particles. The thresholding method applied was Ridler-Calvard (Ridler and Calvard, 1978) (sensitivity 1.5), and the cube dissection method (cube side length 20) was used for objects declumping.

To understand the precision of the volumetric method, we designed a comparison study of the volumetric analysis using regularly shaped particles, of which the volume can be computed using a simple

geometric equation. We took ten regularly shaped microplastic particles and dyed them to calculate their volumes by Z-Stack CLSM imaging and thereafter BiofilmQ 3D image processing. In contrast, for statistical analysis of the probable volumes of the regularly shaped particles, we measured the 2D orthogonal projection images of the same particles (ellipsoid and cylinder shaped) using the ImageJ software (Version: 1.53f51 National Institutes of Health, Bethesda, MD, USA). We first set a known scale for the measurement in ImageJ. Thereafter, we took multiple measurements ($n > 10$) for each height and width of every 2D orthogonal projections generated from various 3D particles. We conducted a Monte Carlo simulation using a uniform distribution between the measured maximum and minimum values for each of the height and radius (i.e., max height – min height and max radius – min radius) of each particle to calculate the probable median value of the volume. Crystal Ball (11.1.2.4.600) software from Oracle (Austin, TX, USA) was used for the Monte Carlo simulation.

The newly developed volumetric measurement procedure was thereafter applied on artificial soil mixture with spiked microplastics and probable organic contaminants. Mortar and pestle-ground wood and plant biomass (0.025 g), mortar and pestle-ground shrimp shell (0.025 g), and microplastic mix (0.05 g) were spiked in 500 g artificial soil (100 ppm w/w microplastic concentration). Microplastics and

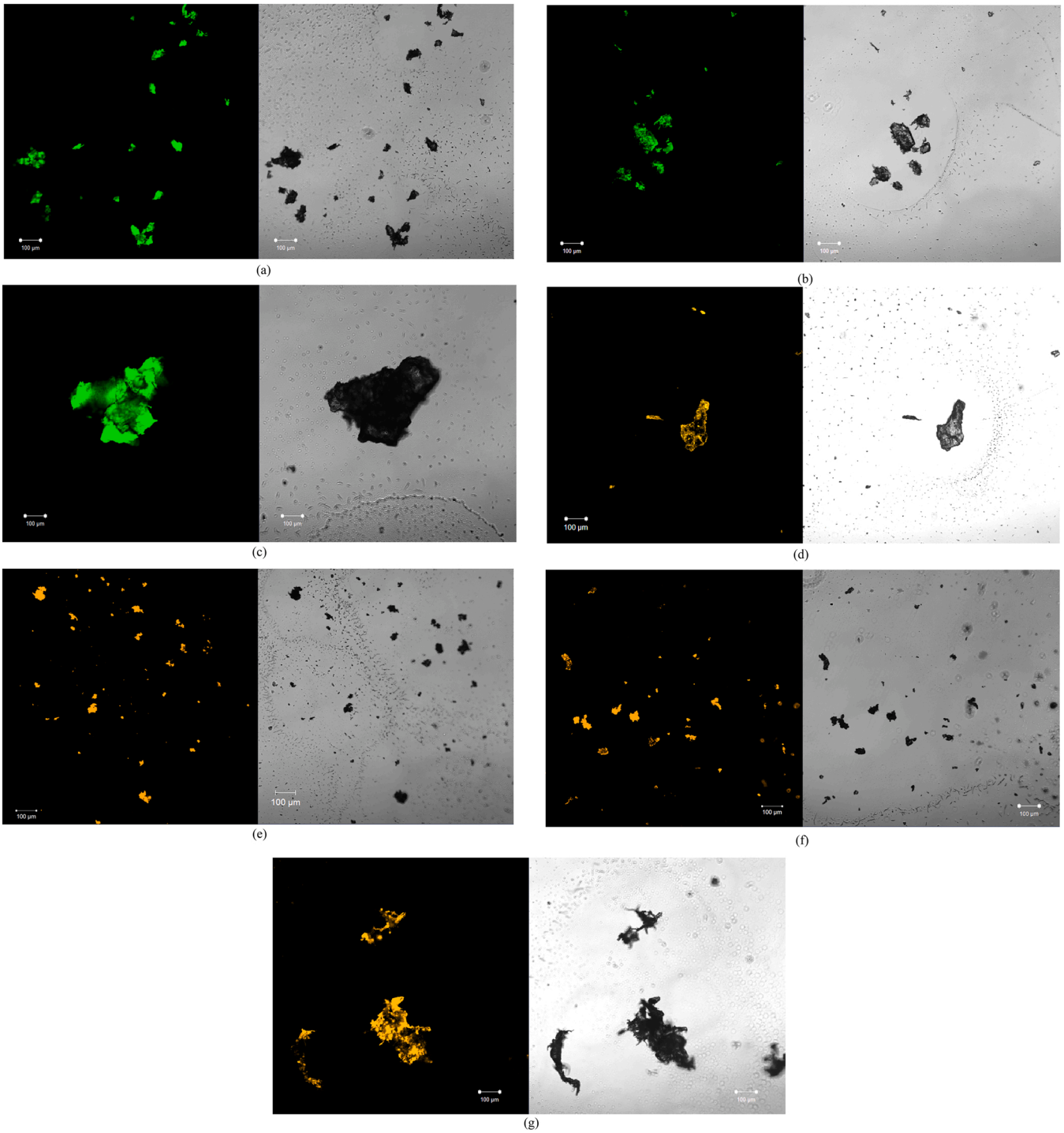

Fig. 1. Nile Red detection of different microplastic types (single focus imaging). (a) LDPE, (b) HDPE, (c) PP, (d) PS, (e) EPS, (f) PU, and (g) PVDF.

contaminants spiked in the artificial soil mixture underwent density separation prior to dyeing and subsequent fluorescence imaging.

3. Results and discussion

3.1. Detection of microplastics and probable contaminants

The experiment was conducted through four primary detection steps: (i) detection of various microplastic types, (ii) detection of probable contaminations, (iii) detection of various microplastics along with probable contamination mixtures, and (iv) detection of various types of microplastics and differentiating microplastics from spiked probable contaminations inside artificial soil.

The experiment started with the use of Nile Red dye on separate microplastic types to comprehend successful detection. LDPE, HDPE, and PP appeared as green (Ex 488 nm, Em 523 nm); PS, EPS, PU, and PVDF appeared as yellowish orange (Ex 555 nm, Em 585 nm) (Figs. 1 and S2; Supplementary Material). The overall detection rate (based on the known number of spiked particles, recounted under CLSM after dyeing) was > 98%. We also successfully detected the autofluorescence of PET prior to the application of the dye (Ex 400 nm, Em 445 nm) (Fig. S3; Supplementary Material).

The ability to detect various probable contaminations was tested using their respective specified blue dye/dyes-mix (Figs. 2 and S4; Supplementary Material). We used a kitchen-blender to grind anchovy (DAPI testing), shrimp shell (testing of Calcofluor White + Evans Blue on chitin), wood (DAPI testing), green plant/leaves parts (DAPI testing), along with some cotton fiber and paper towel fiber (testing of Calcofluor White + Evans Blue).

Proceeding to the next step of the experiment, we mixed 0.025 g of mortar and pestle-ground wood/plant biomass, along with 0.025 g of mortar and pestle-ground shrimp shell and a 0.05 g microplastic mix (w/w equal mixture of all microplastics used in this study). This mixture was sequentially dyed with Calcofluor White + Evans Blue + DAPI solution and Nile Red. Low-molecular-weight microplastics (green), high-molecular-weight microplastics (yellowish orange), and organic contaminants (ground wood/plant parts and shrimp shell, in blue) are distinctly visible in Figs. 3 **(a, b)** and S5 (a, b), Supplementary Material).

In the final part of the experiment, we intended to detect microplastics from organic contaminants and microplastics spiked in an artificial soil mixture. We spiked mortar and pestle-ground wood and plant biomass (0.025 g), mortar and pestle-ground shrimp shell (0.025 g), and microplastic mixture (0.05 g) in 500 g of artificial soil (100 ppm w/w microplastic concentration). Microplastics and contaminants spiked in the artificial soil mixture underwent density separation prior to fluorescence imaging.

Table 1 summarizes the advantages and disadvantaged of earlier research conducted on microplastic detection from various matrices using Nile Red staining. Almost all the studies suffered challenges caused by false positive detections of microplastics as Nile Red dyed organic remnants. Nile Red overestimated ($p < 0.05$) the microplastic counts, notably in river water samples, despite wet peroxidation pretreatment (Stanton et al., 2019). Some studies used a rapid detection approach (Kang et al., 2020; Maes et al., 2017; Nalbone et al., 2021; Prata et al., 2020) by real-time screening of microplastics from filter plates and by not using high-end instruments such as confocal microscopy. This approach can bypass the efficacy argument for the sake of vastness, sometimes with the help of automated counting software (MP-VAT) (Prata et al., 2019).

Some studies have attempted to increase the detection efficacy using additional techniques such as FTIR, Raman, and hyperspectral imaging (Dowarah et al., 2020; Erni-Cassola et al., 2017; Prata et al., 2021a; Shim et al., 2016). In addition to false positive detections, if identifying the microplastic types is within the scope of the study, additional techniques are sometimes used.

As a co-staining approach for false positive detection, Stanton et al.

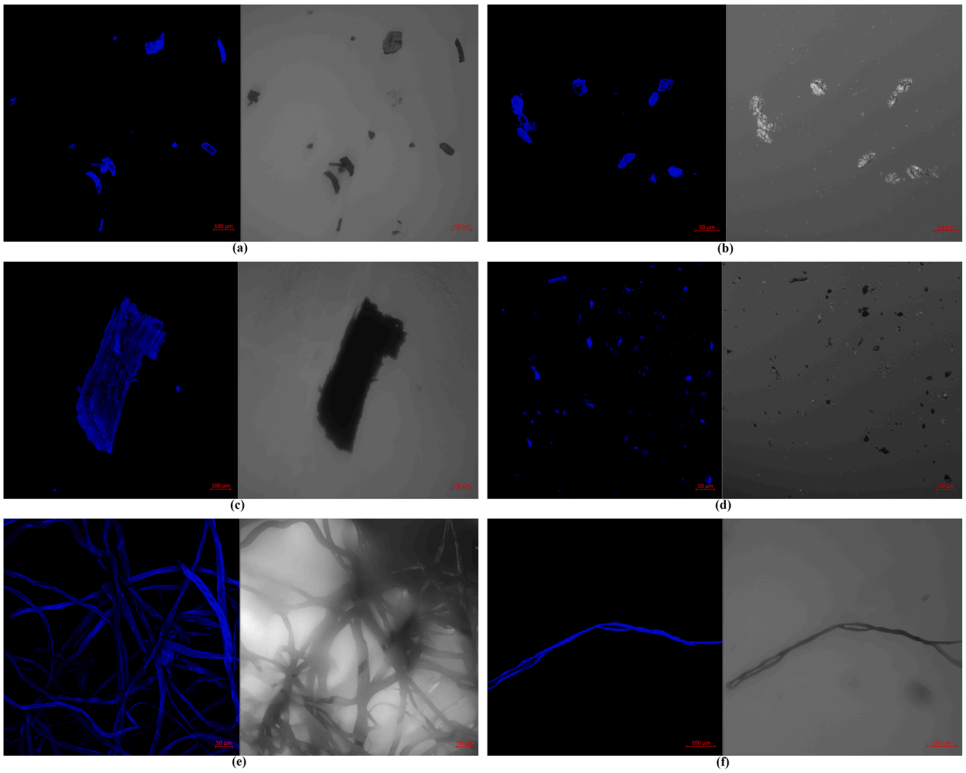

Fig. 2. Testing the components of blue dye mixture on their respective target contaminants (Z-Stack imaging). (a) Ground anchovy, (b) ground shrimp shell, (c) ground wood, (d) crushed green plant/leaves parts, (e) cotton fibers, and (f) paper towel fiber. Fluorescence was induced for chitin of shrimp shell, cotton, and paper fiber using Calcofluor White & Evans Blue solution. Fluorescence of rest of the samples were induced by only using DAPI.

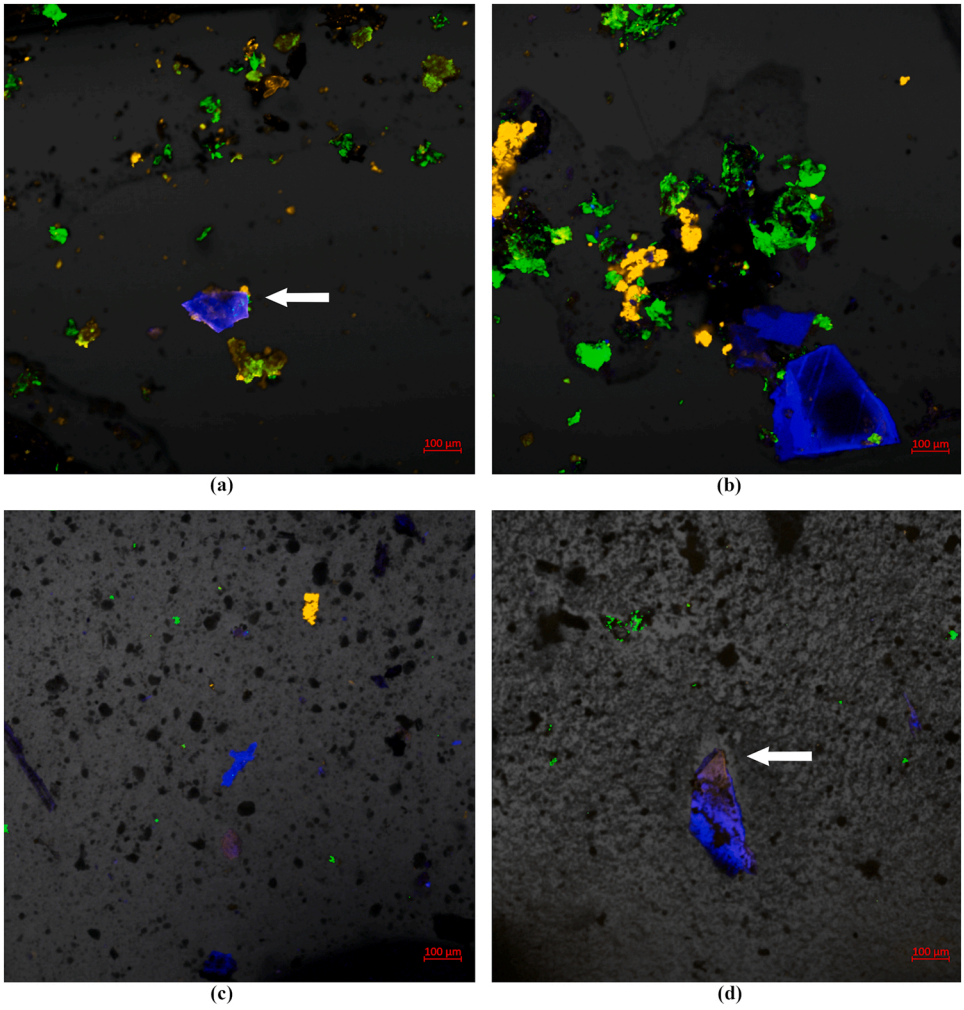

Fig. 3. (a, b) Identification of microplastics from chitin and wood/plant-parts contaminated microplastics mixture. (c, d) Detection of microplastics from organic contamination and spiked microplastic (100 ppm w/w) in artificial soil. We have used the merged view of the fluorescence channels along with the visible light photographic channel (single focus imaging) to demonstrate the specificity to their respective binding agents of the dyes used. LDPE, HDPE, and PP appeared as green; PS, EPS, PU, and PVDF appeared as yellowish orange; organic contaminants (probable false positives) appeared as blue. The white arrow in (a & d) demonstrates how falsely colored organic particle by Nile Red can be detected using blue counterstaining solution.

(Stanton et al., 2019) tested DAPI (0.5 µg mL^{-1}) as a second stain for detecting biological material. However, DAPI at higher concentrations (~10 µg mL^{-1}) was suggested to be used to visualize live cells (alongside dead cells) as it is impermeable to live cell membranes at a lower concentration (~1 µg mL^{-1}) (Biotium, 2019). Another study by Helmberger et al. (Helmberger et al., 2020) used Calcofluor White dye to identify two frequent false positives of the Nile Red method: chitin and cellulose. However, they could not detect UV-induced emission of DAPI through the emission filter alongside Calcofluor White, which could provide a counterstain for a wider range of biological materials. In addition, none of the above studies dealt with volumetric or mass analyses of environmental microplastics.

In this study, we used a higher concentration of DAPI (10 µg mL^{-1}) to ensure the dyeing of all residues of biological origin, irrespective of whether they were dead or alive. After a prolonged session of trial and error, we also managed to establish a sweet spot for excitation/emission wavelengths (excitation 400 nm, emission 435 nm and detection 300–440 nm). This can produce fluorescence and detect both DAPI and Calcofluor White emissions in a single blue fluorescence channel with sufficient brightness (Fig. 2).

3.2. Field study

After the successful completion of microplastic detection in the artificial soil with a recovery rate of over 98%, we used sample soils from agricultural fields. The number of microplastics in each sample (Fig. S7, Supplementary Material), along with the average size of particles in a sample, was calculated using ImageJ and are provided in Table 2. The average particle size for the microplastic samples in mulching agricultural fields was between 54,000 and 270,000 μm^2. The abundance of green fluorescence in the samples rather than orange is explained by the fact that polyethylene is mainly used as a mulch film.

Microplastic particles are relatively more abundant in mulching fields and plastic sheet-covered greenhouses. The fields with a history of mulching were actively mulching less than 1–2 years ago yet showed a lower density of microplastics.

3.3. Comparison of CLSM with FTIR detection of microplastics

The detection capabilities of our method were compared with those of the standard FTIR detection of microplastics. Each sample in Table 3 underwent two detection tests, first FTIR detection, followed by dyeing, and CLSM detection (CLSM detection images in Table. S2; Supplementary Material).

We could not find any noticeable difference between the FTIR and CLSM results for all sample types and pretreatment methods. More precise differentiation among various plastic types in the CLSM method (using more dyes) can be a future endeavor.

3.4. Volumetric analysis

Quantitative assessment of environmental microplastics using existing technologies (FTIR, Raman, fluorescence, etc.) is primarily based on particle counts (number of microplastic particles per unit area

Table 1
Earlier studies on Nile Red detection of microplastics from environmental soil/water or food samples.

Applied Matrices	Pretreatment method	Plastic types	Advantage	Disadvantage	Reference
Net tow and beach sand samples.	30% H_2O_2.	PP, PE, PS, PA-6, PC, PU, PET, PVC.	Variety of plastic types considered.	Only green fluorescence was chosen for detection as the study does not include false positive detections, and natural contaminants fluoresced in red.	(Erni-Cassola et al., 2017)
Quartz sand, eggs of sea snail, a piece of wood, cellulose tissue, sea urchin skeleton, sea grass leaf, cuttlefish bone, coralline red algae, and sea snail shells.	None.	PP, PE, PET, PVC.	Comparison and optimization (20 μg mL^{-1} for 10 min) of the existing staining protocols.	Several biological materials like cellulose, sea animal shell, and wood were stained.	(Konde et al., 2020)
Consumer plastics in aquatic environment.	None.	LDPE, PS, PET, PA.	Nile Red fluorescence lifetime analysis provides a simple and sensitive approach for detecting different widely used plastics.	Limited plastic types and no highlight on false detections.	(Sancataldo et al., 2020)
Blue mussels	overnight in 10% KOH (40 g/mL w.v.), constant stirring at 60 ∘C.	PE		Organic residues false positive lead to overestimates.	(Nalbone et al., 2021)
Textile fiber, fresh water and drinking water	30% H_2O_2, 80 °C, 8 h	PES, PA, Acrylic, PE, PP, PVC, EPS, PET etc.	Used DAPI as a co-stain to color the biological false positives.		(Stanton et al., 2019)
Weathering test samples, field sand samples, floating marine samples.	Density separation and wet peroxidation	LDPE, HDPE, PU, PEVA, PP, PVC, PC, PET, EPS, PES, PA.	Quick identification for wide variety of polymer particles in laboratory-controlled samples	Identification efficiency in field samples with organic remnants remained questioned as of false detections.	(Shim et al., 2016)
Cryogrinded lab samples	Density separation and wet peroxidation	PET, HDPE, PVC, LDPE, PP, PS, PA, PU, ABS, PC, PBS.	Effects of wavelength, staining temperature and time, H_2O_2 and NaCl addition on NR staining was optimized.	Addition of H_2O_2 or combined H_2O_2 and NaCl can reduce the risk of false positives from natural organic materials, but the 'dim glow' from chitin was still present.	(Wang et al., 2021)
Invertebrate biomass	30% H_2O_2, 48 h	PE, PP, PVC, EPS	Use of Calcofluor white significantly reduced the false detection of chitin and cellulose.	Use of Calcofluor White does not ensure all organic remnants detection.	(Helmberger et al., 2020)
Mussels	10% KOH, 96 h, 40 °C	PE, PVC, PET, PS	Detection was further tested using Raman spectroscopy on random particles.	No measure taken for false positive detection using Nile Red.	(Dowarah et al., 2020)
Biological samples	10% KOH, 60 °C, 24 h, followed by treatments with boiling water and acetone.	LDPE, HDPE, PP, PVC, PS, EPS, PET	A modified pretreatment digestion efficiency of 97–100% ensures lower false positive.	Acetone can damage plastic's (PVDF, PC, PVC etc.) surface, even dissolve it.	(Prata et al., 2021b)
Marine samples	$ZnCl_2$ density separation.	PA-6, PS, PVC, PET, PE, and PP.	Cross validated and confirmed with FTIR.	Absence of false positive detections	(Maes et al., 2017)
Polymers originated from consumer products & sediment samples.	30% H_2O_2, 48 h, 50 °C.	EPS, HDPE, PP, PA-6, PET, PVC.	Particle pixel brightness threshold limit of 100 a.u., improved the detection of EPS, HDPE, PP, and PA-6; in contrast to the organic components, wood, and chitin.	PET and PVC were not accurately estimated.	(Nel et al., 2021)
Influent and effluent of municipal WWTP	Fenton process & density separation.	PP, PS, and PE.	Almost all available techniques (FTIR, Raman, hyperspectral imaging, stereomicroscope, scanning electron microscopy, and ICP-AES) for microplastic detection were compared with Nile Red detection.	False positives for Nile Red technology were not detected.	(Nguyen et al., 2021)

of scanning). While particle count cannot produce precise volume/mass quantification, a higher level of details on particle size and shape often helps in risk assessment (Primpke et al., 2020). Nevertheless, pyro-GC/MS can directly quantify the mass of microplastics in environmental samples based on the calibration curves of index chemicals (Jung et al., 2021). The capability to quantify microplastics in environmental samples using pyro-GC/MS has been demonstrated in earlier studies (Fischer and Scholz-Böttcher, 2019, 2017; Gomiero et al., 2019; Kirstein et al., 2021). However, to establish a basic method, the selection of indicator ions is necessary and tedious for every microplastic type along with representative index chemicals. In addition, various environmental contaminants can overshadow the plastic indicator ions in the chromatogram. Choosing and segregating indicator ions especially becomes difficult in the case of a composite mixture of microplastics and biopolymers. Thus, the quality and reliance of quantitative studies using pyro-GC/MS depend heavily on the features of the environmental samples and the proficiency of the operator. Sometimes, the non-homogeneity of microplastics in an environmental sample can seriously affect the measurement, as the required test-sample quantity is comparatively lower for pyro-GC/MS than that of other techniques.

A relatively new method by measuring the total organic carbon (TOC) of plastic particles to assess the microplastic mass is also helpful for quantification (Hong et al., 2021). Only this method does not provide any information regarding the particle shape, size, and particle types of microplastics.

In this situation, volumetric analysis of environmental microplastics is important when using a relatively easier method. The method described in this study is not only easy and rapid, but also informative with regard to particle shape and size, which are added benefits. Volumetric analysis of environmental microplastics can be more practical for

Table 2
Number of microplastics in each sample (1 g) along with average size of particles in a sample calculated using the ImageJ software from CLSM data.

Sampling site	Number of microplastics	Percentage of microplastics in each scan area [(area of microplastic/total scan area) × 100]	Ratio of plastic and organic material [(green area + orange area)/ blue area]	Average of plastic size (μm^2) [(green area + orange area)/ number of microplastics]
Site 1 greenhouse	115	0.048	0.018	55200
Site 2 mulching field	46	0.037	0.011	107000
Site 3 (center) mulching field	136	0.058	0.063	56500
Site 3 (side) mulching field	56	0.033	0.061	77100
Site 4 (center) mulching field	80	0.038	0.054	62600
Site 4 (side) mulching field	167	0.085	0.039	67400
Site 5 having history of mulching	13	0.027	0.403	270000
Site 6 having history of mulching	39	0.016	0.119	54100

Table 3
Comparison of microplastic detection using FTIR and CLSM.

Sample	Sample wt.	Pretreatment	PE FTIR	PS FTIR	PP FTIR	PET FTIR	Total FTIR	Total CLSM
artificial soil mixture (100 ppm microplastic contamination w/w)	0.0423 g	organic remove + density separation	23	1	10	3	37	39
	0.0052 g		34	1	1	5	41	36
	0.0398 g	density separation	20	1	1	0	22	23
	0.045 g		37	0	0	3	40	38
	0.066 g		30	0	3	2	35	35
wastewater sample	20 mL	organic remove + density separation	0	1	8	3	12	16
	20 mL		5	3	11	10	29	30
blank	open	organic remove + density separation	3	0	1	1	5	5
	close		2	1	2	2	7	5

understanding the actual contamination level, leading to a better understanding of environmental risks.

Volumetric analysis of regularly shaped microplastics is important for establishing the precision of this measurement. Fig. 4 illustrates the comparison between the statistical (Monte-Carlo simulated) and BiofilmQ calculated volumes for ten regularly shaped (ellipsoid and cylinder) microplastic particles. The 3D volumetric analysis by BiofilmQ generated the Visualization Toolkit (.vtk) files, which were post-processed and rendered into 3D models of the particles using open-source ParaView software (version 5.9.1., Kitware, Inc., New York, USA). For regularly shaped microplastic particles, the volumetric results from both methods were comparable, which validates the method to apply on environmental samples.

The procedure for volumetric measurement of regularly shaped microplastic particles depicted in Fig. 4 was subsequently applied to an artificial soil mixture spiked with microplastic and organic contaminants. An area of 2.37 mm^2 was scanned with an image size of 1894 × 1894 pixels. Scaling of each pixel was 1.25 μm × 1.25 μm × 5 μm. Sixteen tiles were imaged and stitched together, with 19 slices/focal planes (90 μm) for each tile. The microplastic volume for each tile was calculated using BiofilmQ and summed up for total microplastic volume (2582526.65 μm^3) (Fig. 5 and Fig. S9 and S10; Supplementary Material).

4. Conclusion

The conclusions of the current study can be explained in the following form:

I. Chitin, wood lignin, lipids, and cellulosic particles can be stained with Nile Red and remain false positive in the detection method. Lowering this false positive in the classical Nile Red staining method is one of the most challenging parts. We successfully used three water-based dyes, Calcofluor White, Evans Blue, and DAPI together for the first time to eliminate the most probable false detections.
II. Using a threshold-based 3D segmentation procedure (BiofilmQ) on acquired Z-stack confocal images of microplastics, we can assess the microplastic volume and render the 3D model in the Visualization Toolkit (VTK) format. This volumetric measurement of microplastics in environmental and food matrices is extremely helpful to properly assess the contamination level. All existing methods for microplastic detection in the environment provide numerical measurements (except pyro-GC/MS) of microplastics present in the matrix, which often leads to the misunderstanding of the true level of microplastic pollution.
III. The differential staining method is extremely specific to microplastics, such that only simple density separation ($ZnCl_2$) can be a 'good-to-go' pretreatment step for this method. Rapid detection is possible with a shorter pretreatment time. In the case of fine-tuned volumetric measurement of microplastics, a more extensive classical wet peroxidation method can be used.
IV. Due to the high magnification (100X) of the CLSM instrument, we can even detect microplastics of approximately 1 μm in size, which is much more important in terms of adverse effects of microplastics in the environment. The identification of microplastics in this size range should be further investigated.

Supplementary material

Plant part and wood lignin dyed using propidium iodide (single focus imaging). Nile Red detection of different microplastic types (single focus imaging). Autofluorescence of non-stained PET. Testing the components of blue dye mix on their respective target contaminants (Z-Stack imaging). Identification of microplastics from chitin and wood/plant-parts contaminated microplastics mixture and detection of microplastics

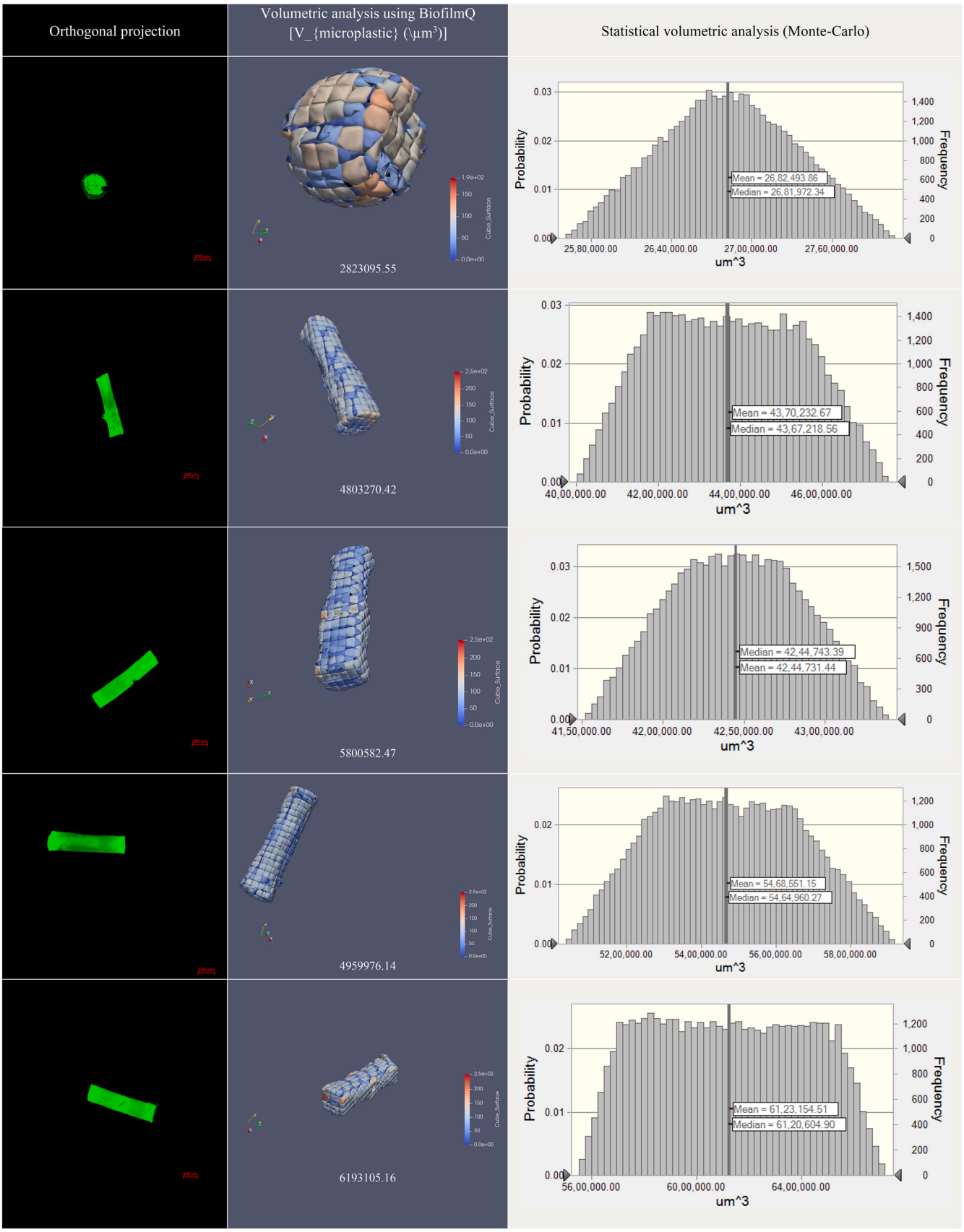

Fig. 4. Comparison of the volumetric measurement of regularly shaped microplastics using the BiofilmQ method and statistical (Monte-Carlo simulation) analysis.

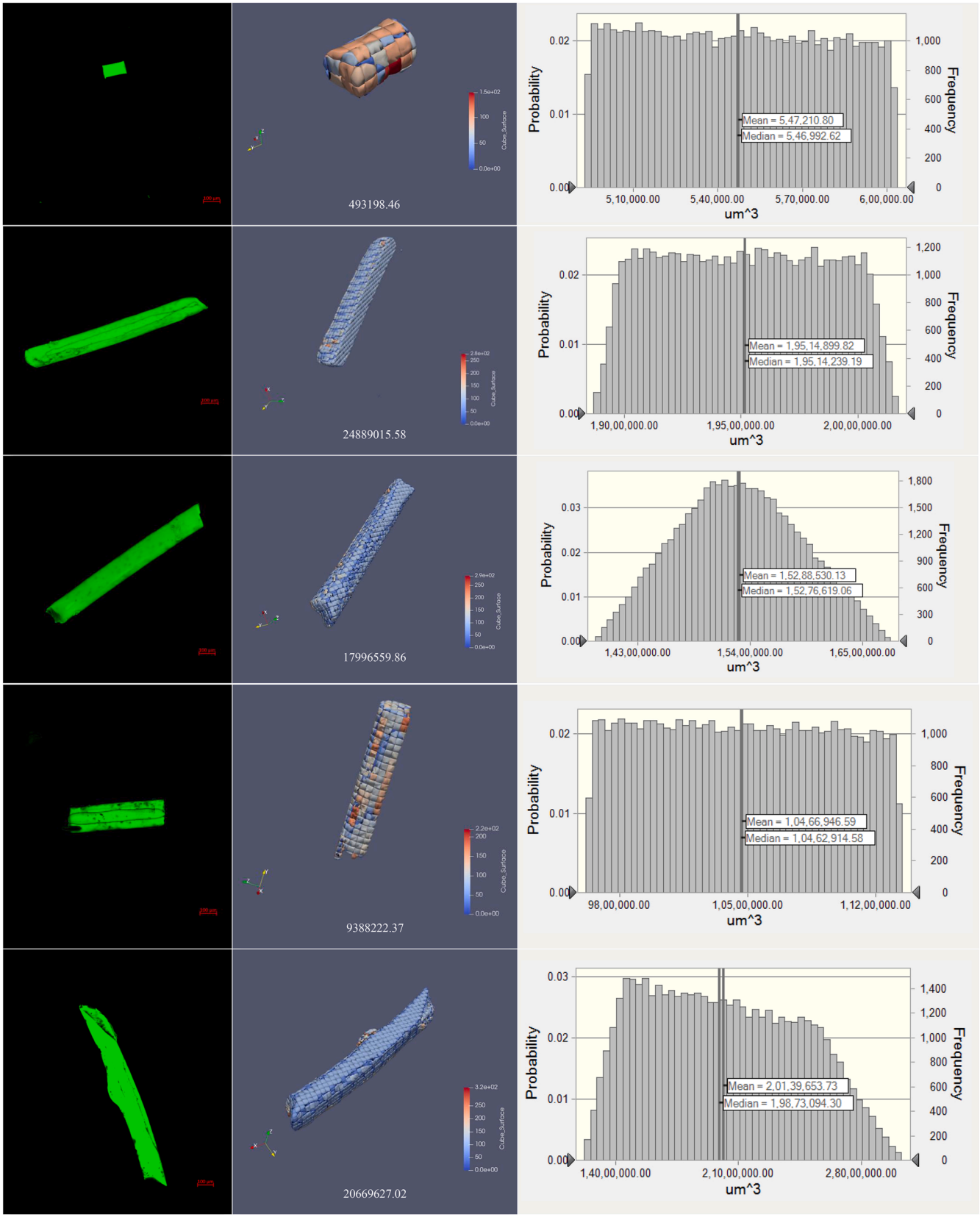

Fig. 4. (*continued*).

from organic contamination and microplastic spiked (100 ppm w/w) artificial soil. Map of agricultural soil sampling area (Bongamri, Paju city, Gyeonggi-do, South Korea). Detection of microplastics in agriculture field soil sample using Nile red method, CLSM images of environmental samples. Wastewater sampling area map. Orthogonal projection of microplastic in artificial soil. BiofilmQ generated.vtk files

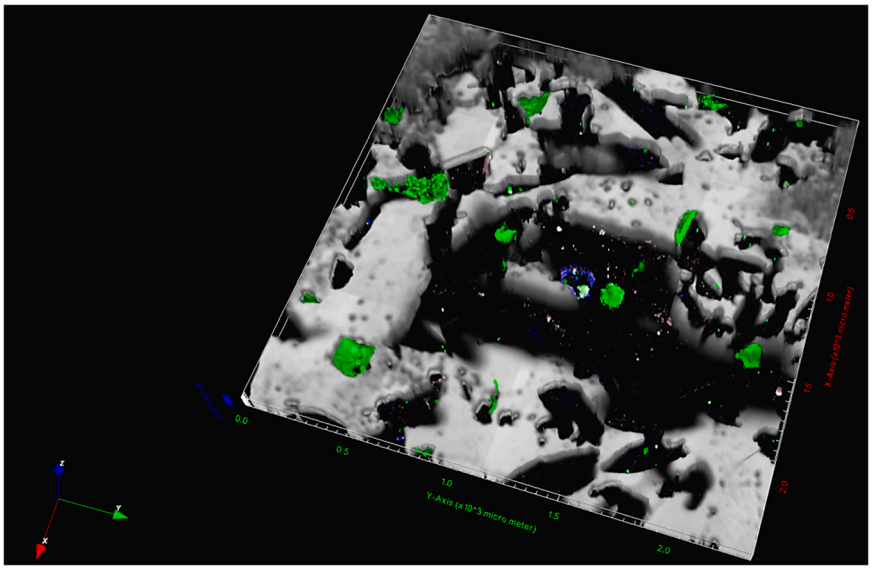

Fig. 5. Z-stack 3D volumetric measurement of microplastic in an artificial soil (16 tiles and ~20 slices for each tile). The.czi file was directly rendered to 3D VTK using Icy 2.3 (Institut Pasteur, Paris, France) software. BiofilmQ calculated total microplastic volume was 2582526.65 μm^3. The two-dimensional orthogonal projection image and the 3D volumetric analysis images are in Figs. S9 and S10, Supplementary Material, respectively.

rendered using Paraview. Spectral reference database used in FTIR detection. Comparison of microplastic detection using FTIR and CLSM.

Funding sources

This work was supported by the National Research Foundation of Korea (NRF) grants funded by the Korean government (MEST) [grant numbers 2020R1A2C2009244 & 2021R1I1A1A01059838] and the Korea Environment Industry & Technology Institute (KEITI) through the Measurement and Risk Assessment Program for Management of Microplastics Program, funded by the Korea Ministry of Environment (MOE) [grant number 2020003110005].

CRediT authorship contribution statement

Abhrajyoti Tarafdar: Conceptualization, Data curation, Investigation, Methodology, Writing – original draft. **Sang-Hyun Choi:** Investigation, Methodology, Writing – original draft. **Jung-Hwan Kwon:** Conceptualization, Supervision, Funding acquisition, Writing – review & editing.

Declaration of Competing Interest

Authors declare no conflicting interests.

Acknowledgements

The authors are thankful to Mr. Minho Jo, Division of Environmental Science and Ecological Engineering, Korea University, for agricultural soil sampling; Mr. Jinwoo Kim, Division of Environmental Science and Ecological Engineering, Korea University, for arranging the reference microplastic particles and Mr. Ja-yun Lim, Center for Analytical and Life Science Instruments, College of Life Sciences & Biotechnology, Korea University, for valuable suggestions regarding confocal microscopy.

Appendix A. Supporting information

Supplementary data associated with this article can be found in the online version at doi:10.1016/j.jhazmat.2022.128755.

References

Alfonso, M.B., Takashima, K., Yamaguchi, S., Tanaka, M., Isobe, A., 2021. Microplastics on plankton samples: Multiple digestion techniques assessment based on weight, size, and FTIR spectroscopy analyses. Mar. Pollut. Bull. 173, 113027 https://doi.org/10.1016/J.MARPOLBUL.2021.113027.

Biotium, 2019. Product Information: DAPI. ⟨https://biotium.com/wp-content/uploads/2016/12/PI-DAPI.pdf⟩.

Dowarah, K., Patchaiyappan, A., Thirunavukkarasu, C., Jayakumar, S., Devipriya, S.P., 2020. Quantification of microplastics using Nile Red in two bivalve species Perna viridis and Meretrix meretrix from three estuaries in Pondicherry, India and microplastic uptake by local communities through bivalve diet. Mar. Pollut. Bull. 153, 110982 https://doi.org/10.1016/j.marpolbul.2020.110982.

Erni-Cassola, G., Gibson, M.I., Thompson, R.C., Christie-Oleza, J.A., 2017. Lost, but found with nile red: a novel method for detecting and quantifying small microplastics (1 mm to 20 μm) in environmental samples. Environ. Sci. Technol. 51, 13641–13648. https://doi.org/10.1021/acs.est.7b04512.

Fischer, M., Scholz-Böttcher, B.M., 2017. Simultaneous trace identification and quantification of common types of microplastics in environmental samples by pyrolysis-gas chromatography-mass spectrometry. Environ. Sci. Technol. 51, 5052–5060. https://doi.org/10.1021/acs.est.6b06362.

Fischer, M., Scholz-Böttcher, B.M., 2019. Microplastics analysis in environmental samples – recent pyrolysis-gas chromatography-mass spectrometry method improvements to increase the reliability of mass-related data. Anal. Methods 11, 2489–2497. https://doi.org/10.1039/C9AY00600A.

Gomiero, A., Øysæd, K.B., Agustsson, T., van Hoytema, N., van Thiel, T., Grati, F., 2019. First record of characterization, concentration and distribution of microplastics in coastal sediments of an urban fjord in south west Norway using a thermal degradation method. Chemosphere 227, 705–714. https://doi.org/10.1016/j.chemosphere.2019.04.096.

Hartmann, R., Jeckel, H., Jelli, E., Singh, P.K., Vaidya, S., Bayer, M., Rode, D.K.H., Vidakovic, L., Díaz-Pascual, F., Fong, J.C.N., Dragoš, A., Lamprecht, O., Thöming, J. G., Netter, N., Häussler, S., Nadell, C.D., Sourjik, V., Kovács, Á.T., Yildiz, F.H., Drescher, K., 2021. Quantitative image analysis of microbial communities with Biofilm. Q. Nat. Microbiol. 6, 151–156. ⟨https://doi.org/10.1038/s41564-020-00817-4⟩.

Helmberger, M., Melinda, S., K, F, Matthew, G., 2020. Counterstaining to separate Nile Red-stained microplastic particles from terrestrial invertebrate biomass. Environ. Sci. Technol. 54, 5580–5588. https://doi.org/10.1021/acs.est.0c00711.

Hong, Y., Oh, J., Lee, I., Fan, C., Pan, S.Y., Jang, M., Park, Y.K., Kim, H., 2021. Total-organic-carbon-based quantitative estimation of microplastics in sewage. Chem. Eng. J. 423, 130182 https://doi.org/10.1016/j.cej.2021.130182.

Ishimura, T., Iwai, I., Matsui, K., Mattonai, M., Watanabe, A., Robberson, W., Cook, A.M., Allen, H.L., Pipkin, W., Teramae, N., Ohtani, H., Watanabe, C., 2021. Qualitative and quantitative analysis of mixtures of microplastics in the presence of calcium carbonate by pyrolysis-GC/MS. J. Anal. Appl. Pyrolysis 157, 105188. https://doi.org/10.1016/J.JAAP.2021.105188.

Jung, S., Cho, S.H., Kim, K.H., Kwon, E.E., 2021. Progress in quantitative analysis of microplastics in the environment: a review. Chem. Eng. J. 422, 130154 https://doi.org/10.1016/J.CEJ.2021.130154.

Kang, H., Park, S., Lee, B., Ahn, J., Kim, S., 2020. Modification of a nile red staining method for microplastics analysis: a nile red plate method. Water 12, 3251. https://doi.org/10.3390/w12113251.

Kirstein, I.V., Hensel, F., Gomiero, A., Iordachescu, L., Vianello, A., Wittgren, H.B., Vollertsen, J., 2021. Drinking plastics? – Quantification and qualification of microplastics in drinking water distribution systems by μFTIR and Py-GCMS. Water Res. 188, 116519 https://doi.org/10.1016/j.watres.2020.116519.

Konde, S., Ornik, J., Prume, J.A., Taiber, J., Koch, M., 2020. Exploring the potential of photoluminescence spectroscopy in combination with Nile Red staining for microplastic detection. Mar. Pollut. Bull. 159, 111475 https://doi.org/10.1016/j.marpolbul.2020.111475.

Leung, M.M.L., Ho, Y.W., Lee, C.H., Wang, Y., Hu, M., Kwok, K.W.H., Chua, S.L., Fang, J. K.H., 2021. Improved Raman spectroscopy-based approach to assess microplastics in seafood. Environ. Pollut. 289, 117648 https://doi.org/10.1016/j.envpol.2021.117648.

Lin, J., Xu, X.P., Yue, B.Y., Li, Y., Zhou, Q.Z., Xu, X.M., Liu, J.Z., Wang, Q.Q., Wang, J.H., 2021. A novel thermoanalytical method for quantifying microplastics in marine sediments. Sci. Total Environ. 760, 144316 https://doi.org/10.1016/j.scitotenv.2020.144316.

Liu, Y., Li, R., Yu, J., Ni, F., Sheng, Y., Scircle, A., Cizdziel, J.V., Zhou, Y., 2021. Separation and identification of microplastics in marine organisms by TGA-FTIR-GC/MS: A case study of mussels from coastal China. Environ. Pollut. 272, 115946 https://doi.org/10.1016/J.ENVPOL.2020.115946.

Luo, Y., Gibson, C.T., Chuah, C., Tang, Y., Naidu, R., Fang, C., 2021. Applying Raman imaging to capture and identify microplastics and nanoplastics in the garden. J. Hazard. Mater., 127788 https://doi.org/10.1016/J.JHAZMAT.2021.127788.

Lv, L., Qu, J., Yu, Z., Chen, D., Zhou, C., Hong, P., Sun, S., Li, C., 2019. A simple method for detecting and quantifying microplastics utilizing fluorescent dyes - Safranine T, fluorescein isophosphate, Nile red based on thermal expansion and contraction property. Environ. Pollut. 255. https://doi.org/10.1016/j.envpol.2019.113283.

Maes, T., Jessop, R., Wellner, N., Haupt, K., Mayes, A.G., 2017. A rapid-screening approach to detect and quantify microplastics based on fluorescent tagging with Nile Red. Sci. Rep. 7, 1–10. https://doi.org/10.1038/srep44501.

Nalbone, L., Panebianco, A., Giarratana, F., Russell, M., 2021. Nile Red staining for detecting microplastics in biota: preliminary evidence. Mar. Pollut. Bull. 172, 112888 https://doi.org/10.1016/j.marpolbul.2021.112888.

Nel, H.A., Chetwynd, A.J., Kelleher, L., Lynch, I., Mansfield, I., Margenat, H., Onoja, S., Goldberg Oppenheimer, P., Sambrook Smith, G.H., Krause, S., 2021. Detection limits are central to improve reporting standards when using Nile red for microplastic quantification. Chemosphere 263. https://doi.org/10.1016/j.chemosphere.2020.127953.

Nguyen, N.B., Kim, M.K., Le, Q.T., Ngo, D.N., Zoh, K.D., Joo, S.W., 2021. Spectroscopic analysis of microplastic contaminants in an urban wastewater treatment plant from Seoul, South Korea. Chemosphere 263, 127812. https://doi.org/10.1016/j.chemosphere.2020.127812.

OECD, 2010. Test No. 317: Bioaccumulation in Terrestrial Oligochaetes, OECD Guidelines for the Testing of Chemicals, Section 3. OECD Publishing, Paris. ⟨https://doi.org/10.1787/9789264090934-en⟩.

Parker, L., 2020. Plastic trash flowing into the seas will nearly triple by 2040 without drastic action. Natl. Geogr. Mag. 2020–2022.

Picó, Y., Barceló, D., 2020. Pyrolysis gas chromatography-mass spectrometry in environmental analysis: Focus on organic matter and microplastics. TrAC Trends Anal. Chem. 130, 115964 https://doi.org/10.1016/J.TRAC.2020.115964.

Piyawardhana, N., Weerathunga, V., Chen, H.-S., Guo, L., Huang, P.-J., Ranatunga, R.R. M.K.P., Hung, C.-C., 2022. Occurrence of microplastics in commercial marine dried fish in Asian countries. J. Hazard. Mater. 423, 127093 https://doi.org/10.1016/J.JHAZMAT.2021.127093.

Plastics Europe & EPRO, 2021. Plastics - the Facts 2021: An analysis of European plastics production, demand and waste data 34. ⟨https://plasticseurope.org/knowledge-hub/plastics-the-facts-2021/⟩.

Prata, J.C., Reis, V., Matos, J.T.V., da Costa, J.P., Duarte, A.C., Rocha-Santos, T., 2019. A new approach for routine quantification of microplastics using Nile Red and automated software (MP-VAT). Sci. Total Environ. 690, 1277–1283. https://doi.org/10.1016/j.scitotenv.2019.07.060.

Prata, J.C., Alves, J.R., da Costa, J.P., Duarte, A.C., Rocha-Santos, T., 2020. Major factors influencing the quantification of Nile Red stained microplastics and improved automatic quantification (MP-VAT 2.0). Sci. Total Environ. 719. https://doi.org/10.1016/j.scitotenv.2020.137498.

Prata, J.C., da Costa, J.P., Fernandes, A.J.S., da Costa, F.M., Duarte, A.C., Rocha-Santos, T., 2021a. Selection of microplastics by Nile Red staining increases environmental sample throughput by micro-Raman spectroscopy. Sci. Total Environ. 783, 146979 https://doi.org/10.1016/J.SCITOTENV.2021.146979.

Prata, J.C., Sequeira, I.F., Monteiro, S.S., Silva, A.L.P., da Costa, J.P., Dias-Pereira, P., Fernandes, A.J.S., da Costa, F.M., Duarte, A.C., Rocha-Santos, T., 2021b. Preparation of biological samples for microplastic identification by Nile Red. Sci. Total Environ. 783, 147065 https://doi.org/10.1016/j.scitotenv.2021.147065.

Primpke, S., Fischer, M., Lorenz, C., Gerdts, G., Scholz-Böttcher, B.M., 2020. Comparison of pyrolysis gas chromatography/mass spectrometry and hyperspectral FTIR imaging spectroscopy for the analysis of microplastics. Anal. Bioanal. Chem. 412, 8283–8298. https://doi.org/10.1007/s00216-020-02979-w.

Ridler, T.W., Calvard, S., 1978. Picture thresholding using an interactive selection method. IEEE Trans. Syst. Man Cybern. 630–632. https://doi.org/10.1109/TSMC.1978.4310039 (smc-8).

Sancataldo, G., Avellone, G., Vetri, V., 2020. Nile Red lifetime reveals microplastic identity. Environ. Sci. Process. Impacts 22, 2266–2275. https://doi.org/10.1039/d0em00348d.

Shim, W.J., Song, Y.K., Hong, S.H., Jang, M., 2016. Identification and quantification of microplastics using Nile Red staining. Mar. Pollut. Bull. 113, 469–476. https://doi.org/10.1016/j.marpolbul.2016.10.049.

Shruti, V.C., Pérez-Guevara, F., Roy, P.D., Kutralam-Muniasamy, G., 2022. Analyzing microplastics with Nile Red: emerging trends, challenges, and prospects. J. Hazard. Mater. https://doi.org/10.1016/j.jhazmat.2021.127171.

Sridhar, A., Kannan, D., Kapoor, A., Prabhakar, S., 2022. Extraction and detection methods of microplastics in food and marine systems: a critical review. Chemosphere 286, 131653. https://doi.org/10.1016/J.Chemosphere.2021.131653.

Stanton, T., Johnson, M., Nathanail, P., Gomes, R.L., Needham, T., Burson, A., 2019. Exploring the efficacy of Nile Red in microplastic quantification: a costaining approach. Environ. Sci. Technol. Lett. 6, 606–611. https://doi.org/10.1021/acs.estlett.9b00499.

Tarafdar, A., Lee, J.U., Jeong, J.E., Lee, H., Jung, Y., Oh, H., Bin, Woo, H.Y., Kwon, J.H., 2021. Biofilm development of Bacillus siamensis ATKU1 on pristine short chain low-density polyethylene: a case study on microbe-microplastics interaction. J. Hazard. Mater. 409, 124516 https://doi.org/10.1016/j.jhazmat.2020.124516.

Uurasjärvi, E., Sainio, E., Setälä, O., Lehtiniemi, M., Koistinen, A., 2021. Validation of an imaging FTIR spectroscopic method for analyzing microplastics ingestion by Finnish lake fish (Perca fluviatilis and Coregonus albula). Environ. Pollut. 288, 117780 https://doi.org/10.1016/J.ENVPOL.2021.117780.

Veerasingam, S., Ranjani, M., Venkatachalapathy, R., Bagaev, A., Mukhanov, V., Litvinyuk, D., Mugilarasan, M., Gurumoorthi, K., Guganathan, L., Aboobacker, V.M., Vethamony, P., 2020. Contributions of Fourier transform infrared spectroscopy in microplastic pollution research: a review, 51, 2681–2743 ⟨https://doi.org/10.1080/10643389.2020.1807450⟩.

Wang, Chun, Jiang, L., Liu, R., He, M., Cui, X., Wang, Changhai, 2021. Comprehensive assessment of factors influencing Nile red staining: Eliciting solutions for efficient microplastics analysis. Mar. Pollut. Bull. 171, 112698 https://doi.org/10.1016/j.marpolbul.2021.112698.

World Economic Forum, 2016. The new plastics economy: Rethinking the future of plastics. Ellen MacArthur Found. 120. ⟨https://emf.thirdlight.com/link/faarmdpz93ds-5vmvdf/@/preview/1?o⟩.

Ye, Y., Yu, K., Zhao, Y., 2021. The development and application of advanced analytical methods in microplastics contamination detection: a critical review. Sci. Total Environ., 151851 https://doi.org/10.1016/J.SCITOTENV.2021.151851.